Journal of Sciences, Islamic Republic of Iran 20(2): 115-126 (2009) http://jsciences.ut.ac.ir
University of Tehran, ISSN 1016-1104

Chemical Variation of Tourmaline and Source of Hydrothermal Solutions in Nezam Abad W-(Sn) Ore Deposit, Sanandaj-Sirjan Zone, West-Central Iran

M.A. Nekouvaght Tak[1,*] and K. Bazargani-Guilani[2]

[1]*GeosMining Minerals Consultants, Suit 301, 68 Alfred Street, Milsons Point, NSW 2061, Australia*
[2]*Department of Geology, Faculty of Sciences, University of Tehran, Tehran 14155-6455, Islamic Republic of Iran*

Received: 10 November 2007 / Revised: 11 November 2008 / Accepted: 29 November 2008

Abstract

Tourmalinization characterizes the most pervasive alteration type in the Nezam Abad ore deposit, west-central Iran. It delineates high-temperature centers of mineralization and together with quartz and cassiterite form inner parts of the alteration halo. The composition of tourmalines plots mostly along and between the proton and alkali-deficient end members. Tourmaline in quartzdioritic host is chemically and optically homogenous, with a general tendency toward more schorlitic compositions and is marked by Al deficiency in R3. Tourmaline in hydrothermal veins shows fine-scale chemical and optical zonation, tendency to more dravitic compositions and is characterized by lower F content and larger Fe/(Fe+Mg) variation with generally lesser values than quartzdioritic counterpart. The Rb-Sr and Sm-Nd isotope analyses of quartzdioritic units of the Boroujerd complex and separated hydrothermal tourmalines (εNd -6.43 to -3.24) imply derivation from enriched sources with a lower Sm/Nd ratio than Chondritic Uniform Reservoir. The $\delta^{18}O$ values (11.9 to 13.8‰) of quartz of hydrothermal veins suggest magmatic mineralizing fluids whose $\delta^{18}O$ values have been increased through subsequent interaction with metamorphic country rocks. The range of $\delta^{11}B$ values determined for hydrothermal tourmalines are relatively wide and falls at the lighter end of the range for typical continental crust.

Keywords: Tourmaline; Chemical variation; Nezam Abad; Sanandaj-Sirjan zone; West-central Iran

Introduction

Tourmaline is an important gangue mineral in many granitoid-related metal deposits. The best known occurrences of tourmaline with hydrothermal ore deposits are those in Sn±W greisens, veins, skarns and replacements. Of these, greisens and veins are the most common type of tourmaline-bearing Sn±W deposits, occurring either within intrusive granites or in adjacent metasedimentary or metavolcanic country rocks. Distribution of tourmaline in metasomatites, stockworks, secondary haloes and stream sediments is commonly

* Corresponding author, Tel.: 0061 (2) 99296868, Fax: 0061 (2) 99231112, E-mail: nekouvaght@gmail.com

much greater than the dimentions of the ore bodies proper, suggesting that it could be useful for geochemical exploration. Being a common mineral for ore fields, its wide range of composition might provide additional insights into the geochemical and geological environment in which the tourmaline formed [21]. Boron reduces the solidus temperature of granitic melts and expands the liquidus field of quartz, decreases the viscosity of the melt and increases the solubility of Sn, W, and related incompatible elements in residual magmatic fluids, especially higher solubility limits of water in melt [23]. This gives rise to important consequences on the development of magmatic-hydrothermal fluids and processes involved in the magmatic-hydrothermal transition.

The Nezam Abad W-(Sn) ore deposit has been already studied in terms of ore genesis [9,13,14,20, 27,31], ore estimation [15,20], geochemical exploration [22], petrology and petrography of the intrusions [2,3,25,29,31] and isotopic considerations [9,14,25,27].

In the field and at microscopic scale, tourmalinization characterizes the most pervasive alteration type in the Nezam Abad mining area. Tourmaline occurs mainly in aplitic dykes and hydrothermal quartz-tourmaline veins and sporadically in quartzdiorite, which seems to be not primary in origin. Study of paragenesis displayed that tourmalinization preceded and overlapped with the main phase of mineralization and continued to late stage. Tourmalinization delineate high-temperature centers of mineralization and together with quartz and cassiterite form inner parts of the alteration halo.

This paper presents electron microprobe data for tourmaline from the Nezam Abad ore deposit and use the chemical variations to elucidate or at least identify some petrologic characteristics of the rocks. Additionally, using stable and radiogenic isotopes, source of hydrothermal veins and igneous rocks have been discussed.

Location and Mine Geology

The Nezam Abad W-(Sn) ore deposit is located in the northern part of the Sanandaj-Sirjan metamorphic-magmatic belt, west-central Iran (Fig. 1a). The development of this belt has been ascribed to the generation of the Tethys Ocean and its subsequent destruction during Cretaceous and Tertiary convergence and continental collision between the Afro-Arabian and the Eurasian plates [1, 12, 26]. The NW-SE trending Sanandaj-Sirjan zone has a length of about 1500 km and a width up to 200 km. The rocks of this zone are mostly of Mesozoic age with Paleozoic rocks rarely exposed except in the southeast where they are common [6]. This zone is characterized by metamorphic and complexly deformed rocks associated with abundant deformed and undeformed plutons in addition to widespread Mesozoic volcanic rocks. This zone is distinguished from Central Iran by nearly total lack of Tertiary volcanism and the poor development of Tertiary deposits in general [32].

The Nezam Abad mining area has been documented in the 1:100,000 Shazand geological Sheet (49°00′-49°30′ N, 33°15′-34°00′), and is situated 4 km southwest of the Nezam Abad village (N 49° 17′E 33° 40′). Geology of the mining area consists mainly of Boroujerd complex (quartzdiorite, granodiorite and granite) surrounded by hornfels and Jurassic phyllites. Diabasic dykes intrude partly these lithologies [27]. The NW-SE trending Boroujerd complex with a surface area of about 200 km^2 is mostly made up of granodiorite, but a varied series of minor intrusions with mostly quartzdioritic composition are scattered in the southern parts and around the Nezam Abad ore deposit. Numerous aplitic dykes and quartz-tourmaline veins intersect main phase Boroujerd complex, particulary quartzdioritic units (Fig. 1b). Pegmatites with simple mineralogy show remarkable development outside the mining area. This complex like two other main intrusions in the Shazand Sheet (Astaneh and Goushe-Davarian), has intruded Jurassic phyllites-slates-schists, giving rise to typical contact metamorphism. The petrogenesis of metamorphic haloes has been discussed in detail by [25]. The quartzdioritic units of the Boroujerd complex, later phase aplitic dykes and quartz-tourmaline veins dominate magmatic manifestation in the Nezam Abad ore deposit (Fig. 2). Aplitic dykes with normally NW-SE trend and thicknesses between 50 cm and 1 m extend parallel to the Zagros chain. The NW-SE trending quartz-tourmaline veins are composed of quartz and tourmaline as the main gangue minerals in addition to scheelite, cassiterite and sulfidic minerals in the mineralized ones. Their thicknesses vary between 0.5 cm and 2 m.

Materials and Methods

This research is based on field study and laboratory analyses. During field work, geology of the mining area with emphasis on mineralization and distribution of alteration in general, and particularly tourmalinization were studied in detail. Sampling included the quartzdioritic rocks and quartz-tourmaline veins of different tunnels and outcrops. Totally, 12 representative samples of quartzdioritic units and aplitic dykes were analyzed by INAA method at Actlabs, Canada, and XRF at "Bundesanstalt fuer Geowissenschaften und

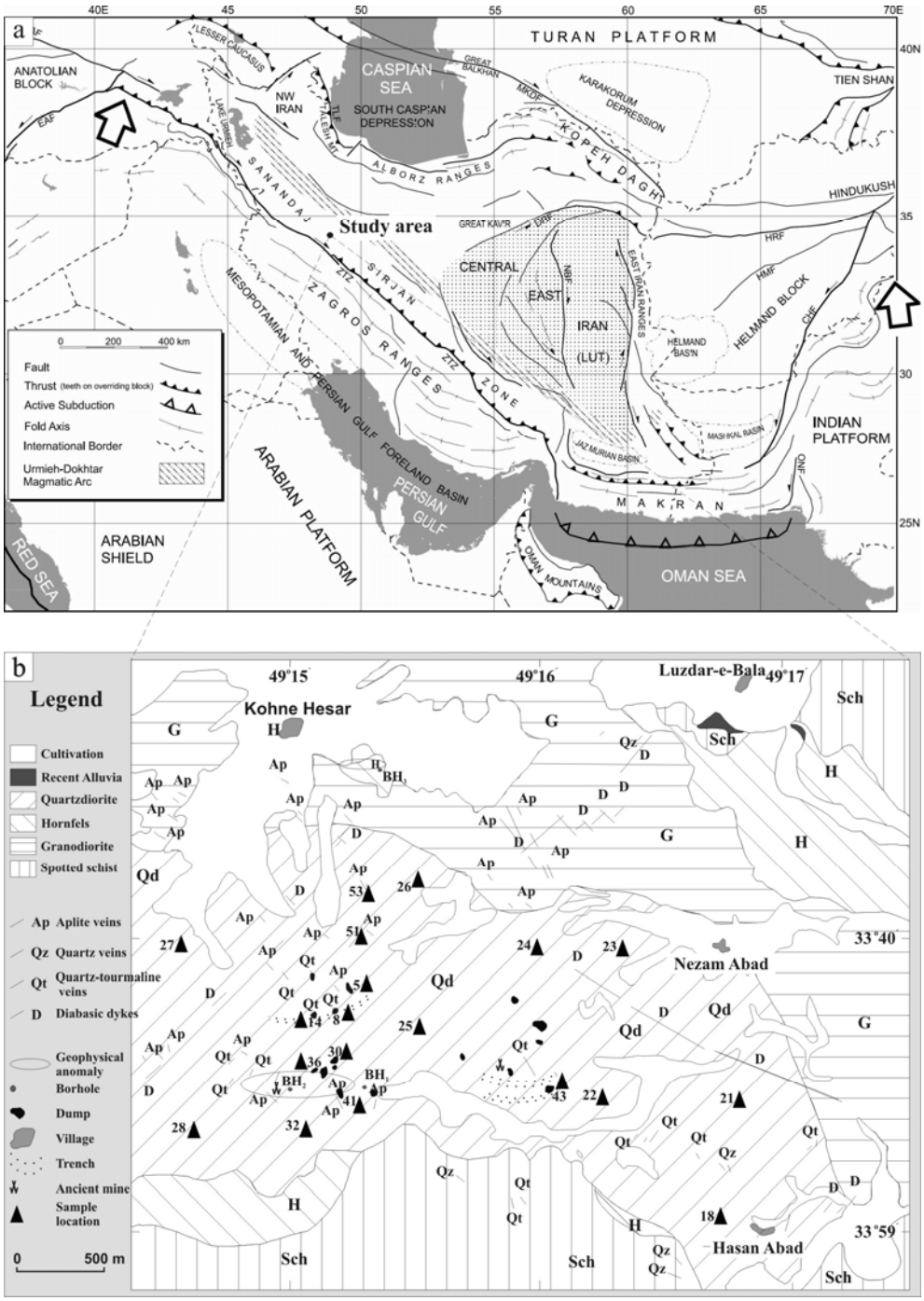

Figure 1. (a) Simplified structural map of Iran and adjacent regions, illustrating location of the study area (modified from Berberian 1981, Jackson and MacKenzie 1984, Alavi 1991). (b) Geological map of the Nezam Abad ore deposit (modified from Nezafati 2006).

Rohstoff, Hannover", Germany. Collectively, 70 polished, polished-thin and thin sections were prepared and studied by conventional petrography microscopes. Detailed electron microprobe analysis was carried out on tourmalines of quartzdioritic host and hydrothermal veins and other ore minerals at Institute of Mineralogy and Mineral Resources of the Technical University of Clausthal, Germany. Isotope analyses including Rb-Sr

and Sm-Nd methods were performed on 7 representative samples, comprising quartzdioritic rocks, aplite and separated hydrothermal tourmalines at Vsegei, St Petersburg, Russia. All isotope measuerments were completed on multicollector mass-spectrometer Tritone TI (Themo) under static mode. In-run correction for mass-bias were done on mass-ratio 146Nd/144Nd=0.7219. Total blank level during analytical processing was not exceeded 0.02 ng for Nd and 0.007 ng for Sm. The international neodimium isotope standard Jndi-1 during analytical period was 143Nd/144 Nd=0.512106+. The stable O isotope analysis was done at Goettingen University, Germany. Samples were analyzed by means of CO_2-laser fluorination. Sample O_2 was analyzed using a Finninigan Deltaplus mass spectrometer in continous flow-mode. The external precision and accuracy per sample is +/− 0.2 permil.

Petrography and Geochemistry of Quartzdioritic Rocks

Field evidence together with geochemical data (Tables 1, 2) indicate that the quartzdioritic units are moderately evolved, metaluminous, calc-alkaline, I-type and belong to the ilmenite series granites. The latter is justified by petrography evidence and measurement of magnetic susceptibility, yielding the range of 0.30-0.33 $*10^{-3}$ SI/unit. This range corroborates with ilmenite-series granites. Mineralogy of these rocks comprises plagioclase (40-50 vol%), biotite (about 20 vol%), quartz (about 10 vol%), hornblende (5-10 vol%), orthoclase and perthite (about 5 vol%), sphene (<1 vol%). Sparse single inclusions of zircon are hosted by other minerals. Tourmaline occurs very rare as anhedral interstitial grains, whose origin seems to be not primary. More details on tourmaline will be given in the next sections.

Very low amount of F, P (Table 1) and B [3,4] of parental magma is an important geochemical signature, evidenced by absence of fluorite, topaz and apatite in hydrothermal veins and very rare amount of tourmaline in quartzdioritic rocks. Apatite was detected only through electron microprobe study as dispersed inclusions in tourmaline. Moreover, low level amounts of litophile metals (e.g. of the Cs-Ta family) (Table 2) indicates weak to moderate degree of differentiation.

Crystal Chemistry of Tourmaline

The general formula of tourmaline is $XY_3Z_6B_3Si_6(O,OH)_{30}$ (OH,F), where common site occupancies include X= Na, Ca, or vacant; Y= Fe^{2+}, Mg, Mn^{2+}, Fe^{3+}, Al, or Li (when coupled with Al); and Z= Al, Fe^{3+}, Mg (when coupled with Ca in X), or $1.33Ti^{4+}$ [23]. The end-members of tourmaline types in terms of their X, Y and Z cations are shown in Table 3.

Exchange vectors were used to represent the composition of tourmaline in a two dimensional projection. The main purposes have been to clarify the chemical variability among the different groups of tourmaline and to apply electron microprobe results to decipher some specific ionic substitutions in the tourmaline. In order to show the chemical variability and exchange vectors, diagrams of [11] and [23] were used. In these diagrams, R1, R2 and R3 are similar to X, Y and Z cations of the tourmaline formula, respectively. Table 4 presents electron microprobe analyses of tourmaline, while Table 5 represents the same data based on atoms p.f.u.

The most common chemical variability where it exists, belongs to the atomic ratio of Fe/(Fe+Mg) which could be designated by the exchange vector $FeMg_{-1}$, relating the compositions of schorl and dravite. Common substitutions in tourmaline groups are uvite [$Ca(Fe,Mg)(NaAl)_{-1}$], ferric Fe^{3+} Al_{-1}, deprotonation $Fe^{3+}O$ $(Fe^{2+}OH)_{-1,}$ the exchange of F for OH, elbaite $LiAlR^{2+}{}_{-2}$ and [(R1) Al][Na (Mg, Fe)$_{-1}$] which generates an alkali-deficient composition (Fig. 3). In this figure, R1= Na+Ca, R2= (Fe_{total}+Mg+Mn^{2+}), R3= (Al+1.33Ti) and $R2^{*}$= FeO+MgO+MnO+Al in R2. For most of the studied samples, the compositions of tourmaline plot along and between the proton and alkali-deficient end members (Fig. 3a). The quantity of Al, as atoms p.f.u. in R2 vs. Fe/(Fe+Mg) indicates the Al deficiency in R3 (value < 0) of an quartzdioritic sample and that the ratio of Fe/(Fe+Mg) decreases from tourmalines of

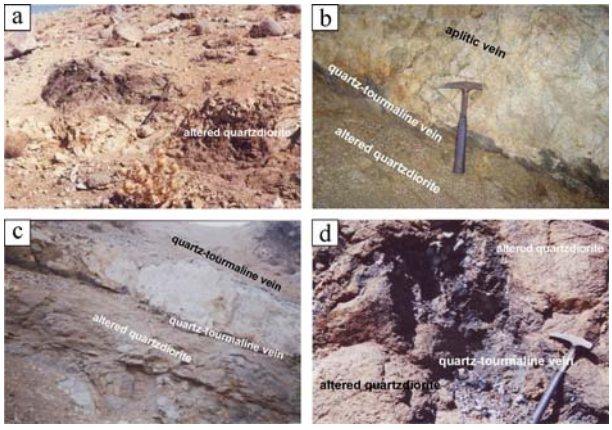

Figure 2. (a) Altered quartzdiorite. (b & c) Altered quartzdiorite cut by aplitic and quartz-tourmaline vein. (d) Quartz-tourmaline vein in altered quartzdiorite, Revesht tunnel.

Table 1. Representative analyses of major elements of the quartzdioritic rocks of the Boroujerd complex. Values are wt%

Sample No.	SiO_2	TiO_2	Al_2O_3	Fe_2O_3	MnO	MgO	CaO	Na_2O	K_2O	P_2O_5	SO_3	Cl	F	LOI	SUM
Main phase															
NZ-18	59.86	0.72	15.83	7.32	0.13	4.04	2.53	2.49	2.51	0.16	<0.01	0.02	0.07	3.64	99.32
NZ-21	57.02	0.82	15.90	7.70	0.14	5.17	5.58	2.46	2.70	0.17	<0.01	0.06	0.13	1.82	99.66
NZ-22	57.30	0.80	15.94	7.92	0.17	4.75	4.83	2.43	2.55	0.15	0.02	0.03	0.08	2.58	99.56
NZ-23	63.24	0.53	15.75	5.73	0.12	2.55	4.50	2.68	2.49	0.12	<0.01	0.03	0.08	1.94	99.74
NZ-24	55.80	0.75	16.04	7.79	0.15	6.22	7.74	2.19	1.70	0.12	<0.01	0.08	0.05	0.98	99.61
NZ-25	55.43	0.78	16.27	8.20	0.15	6.17	7.59	2.20	1.65	0.14	<0.01	0.07	<0.05	0.93	99.59
NZ-26	55.23	0.76	15.99	7.96	0.15	6.34	7.85	2.22	1.66	0.13	<0.01	0.06	<0.05	1.22	99.64
NZ-27	63.16	0.50	15.62	5.67	0.11	2.67	4.26	2.54	2.92	0.10	0.03	0.03	0.06	2.05	99.72
NZ-28	57.87	0.74	15.97	7.31	0.13	5.23	3.19	3.00	2.85	0.15	0.01	0.03	0.05	3.11	99.65
NZ-32	55.32	0.69	16.42	7.81	0.15	5.81	7.85	2.30	1.55	0.14	<0.01	0.06	<0.05	1.48	99.57
Aplite															
NZ-51	73.20	0.07	13.68	0.74	0.02	0.16	0.59	3.54	5.54	0.17	<0.01	0.01	0.06	2.02	99.75
NZ-53	75.00	0.11	13.20	0.87	0.01	0.67	0.75	6.06	0.58	0.13	<0.01	0.01	<0.05	2.44	99.77

Table 2. Trace element analyses of the quartzdioritic rocks of the Boroujerd complex. Values are ppm

Sample No.	Rb XRF	Sr XRF	Ba XRF	Zr XRF	Nb XRF	Sc INAA	La INAA	Ce INAA	Nd INAA	Sm INAA	Cs INAA	Ta INAA	Eu INAA	W INAA	Sn INAA
Main phase															
NZ-18	83	227	584	164	12	24.7	22.0	42	9	4.1	5	<0.5	1.0	<1	<0.01
NZ-21	121	286	462	199	12	22.3	25.7	49	17	4.4	11	<0.5	0.9	<1	<0.01
NZ-22	119	258	404	200	11	21.2	25.4	50	13	4.5	9	<0.5	0.9	<1	<0.01
NZ-23	101	173	296	113	6	21.5	30.5	57	29	4.6	16	<0.5	0.7	4	<0.01
NZ-24	65	306	279	127	4	28.1	20.3	36	17	4.0	5	<0.5	0.9	<1	<0.01
NZ-25	65	304	264	112	8	29.0	20.4	42	19	3.6	6	<0.5	0.9	<1	<0.01
NZ-26	62	307	268	115	6	31.8	21.8	40	20	4.1	7	<0.5	1.2	<1	<0.01
NZ-27	110	156	298	110	8	23.1	30.5	59	29	5.6	10	<0.5	1.0	<1	<0.01
NZ-28	68	185	559	152	7	23.3	30.3	59	22	4.9	<1	<0.5	<0.2	5	<0.01
NZ-32	59	318	256	100	8	31.1	22.5	51	27	5.0	7	<0.5	1.1	4	<0.01
Aplite															
NZ-51	169	95	95	160	15	2.3	6.7	12	<5	1	7	<0.5	0.8	<1	<0.01
NZ-53	15	124	124	185	16	3.8	19.3	46	12	4.1	2	<0.5	0.9	<1	<0.01

quartzdioritic host to hydrothermal veins indicating more affinity to schorl and dravite members of dravite-schorl solid solution, respectively (Fig. 3b). Except one sample, all tourmalines are located under the line ∑(Fe+Mg)=3 confirming Al substitution in R2. The lower amount of Al p.f.u of the sample (NZ-43) also indicates Al deficiency. All studied tourmalines show no elbaite component, as they lie above or along the line of $R2^{*}$= 3 atoms p.f.u (Fig. 3d). Available data show that the composition of tourmalines in quartz-tourmaline veins partly overlaps with the igneous host, but with the following differences:

a) larger variation of Fe/(Fe+Mg), with generally lower values.

b) slightly higher F content (samples NZ-41 & NZ-43).

Chemistry of the Tourmaline Samples

Microscopic study together with electron microprobe

data demonstrated some optical and compositional differences between tourmalines hosted by quartzdiorite and hydrothermal veins. It should be noted that pleochroic color does not always correspond to the chemical composition. In other words, optical zonation which is originated possibly from the variation of Fe^{2+}/Fe^{3+}, does not correlate always with considerable chemical contrast. Conversely, some optically unzoned grains are zoned chemically. Anyway, it is possible to link the pleochroic color and zonation of tourmaline to its mode of formation, i.e. igneous or hydrothermal. Since the changes in pleochroic hue, intensity or zonation are not compatible clearly always with composition, back-scattered electron images were applied to show compositional differences such as relative variations in Fe/(Fe+Mg) and approve if optical zonation correlates with chemical contrast (Figs. 4 and 5).

Tourmaline in Quartzdiorite

Tourmalines show no optical and chemical zonation, occurring very rarely as anhedral interstitial grains that display blue-green color (Fig. 4). There is no sign of any relationships among tourmaline and other AlFeMg minerals. The fluorine content of interstitial tourmaline in quartzdiorite is slightly higher than the detection limit. The ratio of Fe/(Fe+Mg) changes between 0.46 and 0.66 which is higher than the tourmalines in hydrothermal veins (Table 4). Tourmaline, especially solid solution close to the schorl-dravite may be a stable liquidus phase of granitic magmas [5]. In a closed magmatic system P, T and composition vary gradually, so crystalline phases such as tourmaline represent little or no chemical changes. This fact conforms to the tourmaline of the study area. Furthermore, it appears that tourmaline crystallized late in the quartzdiorite of the study area, because it mostly occurs as anhedral interstitial grains.

Tourmaline in Hydrothermal Veins

Tourmaline occurs mostly in quartz-tourmaline veins within the Boroujerd complex. There are no massive tourmaline breccias within granitoid or metamorphosed host rocks or pervasive contact replacements of host rock. Quartz-tourmaline veins of both barren and mineralized types are quartz-rich fracture fillings with massive tourmaline borders and comparatively sharp contacts with the adjacent host quartzdiorite. A general characteristic of vein-associated tourmalines is very complex optical and chemical zonation, which is more obvious in backscattered images than in optical thin sections (Figs. 4, 5). Zonation is mostly oscillatory, but sometimes shows systematic variation in chemical trends from core to rims of the crystals. The ratio of Fe/Fe+Mg varies between 0.35 and 0.48 (Table 5). To confirm any coincidence between optical and chemical zonation, different points of darker and brighter parts along three optically-zoned hydrothermal tourmaline grains were analyzed (Fig. 5 and Table 6). Based on these data, Si, Mn and Cr show no major change and remain mostly constant, while Fe, Ca, Ti and Mg decrease in the darker parts and increase in the brighter parts. Na and Al show the opposite behaviour. Pleochroic color ranges from orange-brown, blue-gray to greenish, and there is no clear correlation between pleochroic color and composition. Figure 6 illustrates tourmalines in igneous host and hydrothermal veins of some of studied samples.

Origin of Hydrothermal Quartz-Tourmaline Veins

The $\delta^{11}B$ values of tourmaline in mineralized and barren hydrothermal veins show the range of -2.7 to -10.56‰ and -6.66 to -8.22‰, respectively [2, 3]. These ranges fall mostly in the lighter end of ranges, typical of continental crust. The field evidence together with geochemical and petrographical data show that the fraction of the melt that attained saturation in tourmaline was very small. This is documented by very low amount of B_2O_3 in quartzdioritic rocks (0.002 to 0.003 wt %) [2, 3] and absence of disseminated tourmalines with fine-scale chemical zonation [17]. More recent experminetal analysis have shown that 2 wt % B_2O_3 at the low end of saturation and possibly > 4 wt % B_2O_3 in melt, require to saturate tourmaline in a hydrous peraluminous felsic liquid [23]. The metaluminous nature and lack of Al activity have also restricted B saturation in the quartzdioritic magma, as B-rich mealuminous granitoids are essentially unknown [23]. The activity of aluminum in melts plays an important role in stability of

Table 3. Tourmaline groups, after [6]

Mineral	X (R1)	Y(R2)	Z (R3)
Elbaite	Na	Al, Li	Al
Olenite	Na	Al	Al
Dravite	Na	Mg	Al
Schorl	Na	Fe^{2+}	Al
Tsilaisite	Na	Al, Mn	Al
Buergerite	Na	Fe^{3+}	Al
Liddicoatite	Ca	Li, Mg	Al
Uvite	Ca	Mg	Al, Mg
Feruvite	Ca	Fe^{2+}	Al, Fe^{3+}, Mg

Table 4. Average electron microprobe analyses of tourmaline hosted by quartzdiorite and quartz-tourmaline veins, Nezam Abad mining area

Sample	Na	Mg	Al	Si	Ca	Ti	Fe	Mn	Fe/ Fe+Mg	Na/ Na+Ca	R1	R2	R1+R2	R3	XAl
NZ-5 n=30	0.461	1.862	6.095	5.853	0.367	0.079	1.015	0.002	0.352	0.553	0.828	2.879	3.707	6.200	0.053
NZ-8 n=15	0.551	1.631	6.510	5.564	0.262	0.132	1.285	0.004	0.440	0.677	0.813	2.920	3.733	6.685	0.249
NZ-14 n=10	0.568	1.412	6.381	5.874	0.205	0.025	1.304	0.000	0.480	0.734	0.773	2.716	3.489	6.414	0.288
NZ-30 n=10	0.561	1.439	6.079	5.943	0.203	0.111	1.335	0.002	0.481	0.734	0.764	2.776	3.540	6.226	0.169
NZ-36 n=7	0.547	1.407	6.361	5.856	0.205	0.025	1.300	0.000	0.480	0.727	0.752	2.707	3.459	6.394	0.250
NZ-41 n=10	0.502	0.755	6.794	5.794	0.092	0.049	1.506	0.000	0.666	0.845	0.594	2.261	2.855	6.859	0.653
NZ-43 n=8	0.534	1.790	5.904	5.813	0.115	0.147	1.534	0.001	0.461	0.821	0.649	3.325	3.974	6.099	-0.080
RV-2 n=6	0.574	1.703	6.089	5.964	0.213	0.562	1.111	0.002	0.394	0.729	0.787	1.687	2.474	6.836	0.800

n: Number of analyzed points in each sample. Except NZ-41 and NZ-43 which are quartzdiorite, the rest samples belong to hydrothermal veins . RV: from Revesht tunnel.

Table 5. Average composition of tourmaline from Nezam Abad. Values are atoms p.f.u, normalized to 24.5 O atoms

Sample	F	Na_2O	MgO	Al_2O_3	SiO_2	CaO	TiO_2	FeO	Cr_2O_3	MnO	B_2O_3	Total	FeO/ FeO+MgO	Na_2O/Na_2O+CaO
NZ-5 n=30	bdl	1.49	7.70	32.1	36.3	2.1	0.66	7.61	0.02	0.05	11.8	100	0.50	0.41
NZ-8 n=15	bdl	1.68	6.40	32.6	37.2	1.4	0.55	9.14	0.03	0.05	10.8	100	0.59	0.54
NZ-14 n=10	bdl	1.80	5.76	33.2	36.0	1.2	0.21	9.60	0.00	0.06	12.2	100	0.63	0.59
NZ-30 n=10	bdl	1.85	5.95	32.0	36.8	1.2	0.92	10.00	0.02	0.05	11.1	100	0.63	0.60
NZ-36 n=7	bdl	1.75	5.76	33.2	36.0	1.2	0.21	9.60	0.00	0.06	12.2	100	0.63	0.59
NZ-41 n=10	0.2	1.67	3.13	35.9	36.0	0.5	0.41	11.30	0.00	0.09	10.9	100	0.78	0.75
NZ-43 n=8	0.2	1.70	7.35	30.9	35.8	0.7	1.21	11.30	0.01	0.08	10.9	100	0.60	0.71
RV-2 n=6	bdl	1.86	7.15	32.5	37.4	1.3	0.47	8.36	0.02	0.04	11.0	100	0.60	0.59

R1= Na+Ca, R2= Fe+Mg+Mn, R3= Al+1.33 Ti, X Al= Al+1.33Ti+Si-12= Al in R2, n= Number of analyzed points in each sample. bdl: Below detection limit which is for F <1000 ppm.

tourmaline. Tourmaline has been found to be unstable in metaluminous biotite-bearing melts with up to 6 wt % B_2O_3 [8], justifying scarcity of tourmaline in the studied quartzdiorites. Nevertheless, it is not possible to rule out the magma itself as a partial source of boron, as quartz-tourmaline veins of both barren and mineralized types are in close association with quartzdioritic units of the Boroujerd complex and the more evolved aplitic dykes. Boron could have accumulated due to incompatible behaviour through magma differentiation, or uptake from country rocks. Based on the above-mentioned points, the second scenario is believed to have played more important role. The same source has been concluded by [25] for tourmaline crystals in the aureoles of Boroujerd complex. Furthermore, field evidence confirms obviously the assimilation of Jurassic phyllites and slates through intrusion of all three main intrusions in the Shazand Sheet, including Astaneh, Boroujerd and Goushe-Davarian. This phenomenon is manifested by contact metamorphism and local very high amounts of

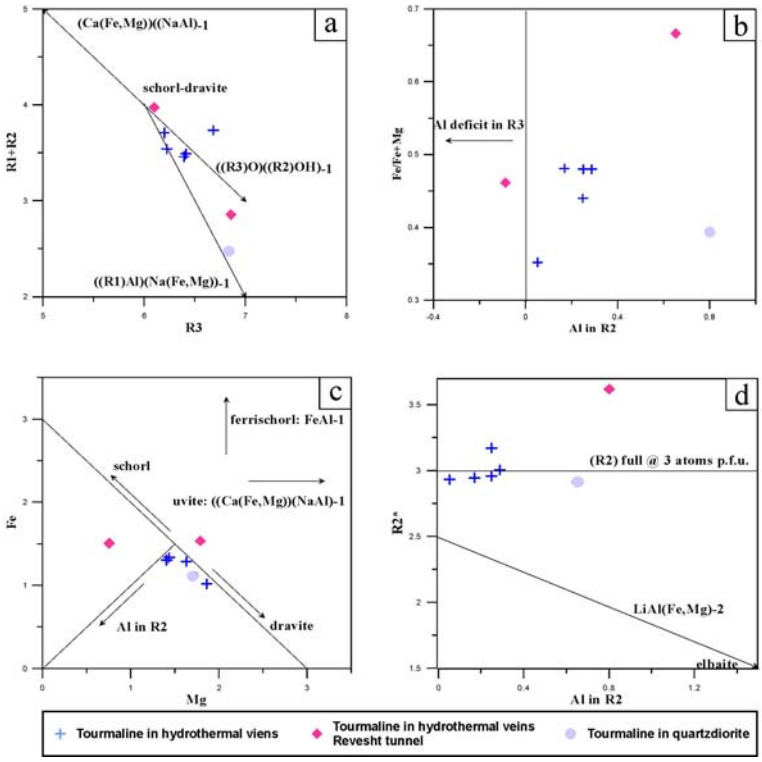

Figure 3. Plots of average cation occupancies of tourmaline from Nezam Abad mining area. (a) The sum of sites R1+R2 vs. R3. (b) Variation of Fe/(Fe+Mg) vs. Al in R2, in which the values of Al in R2 <0 indicate a deficit of Al in R3. (c) Fe/Mg ratio, schorl-dravite plot along the line ∑(Fe+Mg)=3; values of ∑(Fe+Mg) <3 correspond to Al substitution in R2; arrows show regions beyond ∑(Fe+Mg) =3 where dravite and ferrischorl compositions would plot. (d) Occupancy of R2* (FeO+MgO+MnO+Al in R2) vs. Al in R2 in atoms p.f.u. Elbaite lies at R2* = Al in R2 = 1.5; the Li content p.f.u = 3- R2*.

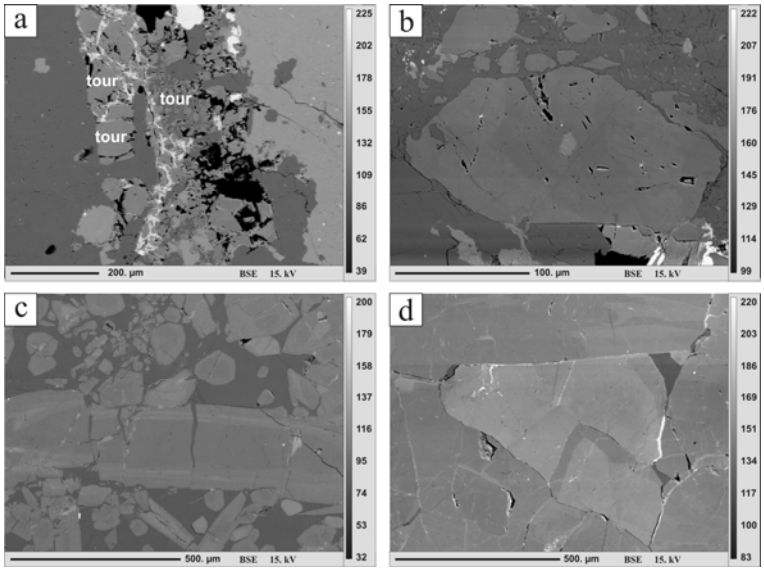

Figure 4. BSE image of tourmaline samples from the Nezam Abad W-(Sn) ore deposit. In order to keep chemical differences, all images have been taken at equivalent contrast and gray levels have not been changed as far as possible. Therefore, gray levels would reflect real chemical differences. (a) Unzoned tourmaline in quartzdiorite (b) Unzoned tourmaline in aplite (c & d) Tourmaline of hydrothermal vein with fine-scale zoning.

biotite, cordierite and andalusite in intrusions. Vigorous assimilation of country rocks by the Boroujerd complex is evidenced also by local graphite occurrences within the intrusion. It is postulated that such occurrences arise from conversion of carbonaceous materials of the country rocks, such as Jurassic schist-phyllite-slate through assimilation by the Boroujerd complex [29]. It has been recognized that < 1 to 2 wt % total FeO+MgO is sufficient to saturate the melts in biotite at temperatures below 800-900^{o}C [17, 18, 28]. Higher whole-rock contents of Fe-Mg components or their crystalline phases, therefore, reflects either that the ferromagnesian phases are at least partially restitic or result from influx of Fe or Mg into the magma system through assimilation, infiltration, etc. [23]. On the other hand, the $\delta^{11}B$ values of the studied hydrothermal tourmalines resemble those of pyroclastic-sedimentary and metavolcanic terrains [2, 3]. Considering presence of such lithologies in the study area, different sources of B through mixing of solutions and interaction with metamorphic country rocks can be envisaged for voluminous tourmalinization in the Nezam Abad ore deposit. In order to constrain source of fluids, the $\delta^{18}O$ values of 5 quartz samples of both mineralized and barren hydrothermal quartz-tourmaline veins were determined (Table 7). These values show the range of 11.9-13.8‰ (ave. 13.4‰), excluding seawater and meteroric water as the candidate sources of hydrothermal fluids. On the contrary, according to data of [16, 30] this range corresponds to the metamorphic or magmatic-metamorphic waters (Fig. 7). The metamorphic waters are attributed to the fluids which have been formed through dehydration of minerals during metamorphism [16]. The $\delta^{18}O$ value of these waters falls in the range of 5 to 25‰, depending to the rock type and fluid/rock interaction during metamorphism [16]. On the other hand, the isotopic signature of magmatic waters is susceptible to change during cooling and isotopic exchange with country rocks and mixing with entrained waters [16]. Furthermore, interaction of magmatic waters with crystalline rocks at higher temperature causes increase of isotopic values. Thus, the $\delta^{18}O$ values of analyzed quartzs (11.9 to 13.8‰) represent magmatic mineralizing fluids whose $\delta^{18}O$ values have been increased following interaction with metamorphic country rocks. In order to clarify the source of quartzdioritic rocks and tourmalines, some samples were analyzed by Sm-Nd and Rb-Sr isotope methods (Table 8 and Fig. 7). The ε_{Nd} was calculated for analyzed samples, using data in literature. The negative ε_{Nd} values of quartzdioritic rocks of the Boroujerd complex and hydrothermal tourmalines imply a magma, derived from a source with a lower Sm/Nd than Chondritic Uniform Reservoir (CHUR). This means that such rocks and associated hydrothermal tourmalines were originated from, or assimilated, old crustal rocks whose, Sm/Nd had been lowered originally when they separated from CHUR. The T_{DM} age model shows Proterozoic age of separation of Nd from depleted reservoir. The Rb-Sr isotope data (initial $^{87}Sr/^{86}Sr$: 0.707 to 0.718) also suggest derivation or strong contamination with continental crust, which is in accordance with Sm-Nd data (Table 8).

Results and Discussion

In this study, the environment and chemistry of tourmaline were utilized in an attempt to underestand the chemical variations in varied environments and possible source of hydrothermal fluids, using O isotope and former B isotope data. Tourmalinization is dominant alteration type in the Nezam Abad W-(Sn) ore deposit, west-central Iran and characterizes the inner parts of the alteration halo. Tourmaline occurs very rare in quartzdioritc igneous host, while together with quartz are the main gangue mineral of hydrothermal veins. Sparse tourmaline grains in quartzdiorite are uniform chemically and optically and tend to schorlitic members of the dravite-schorl solid solution. In contrast, massive

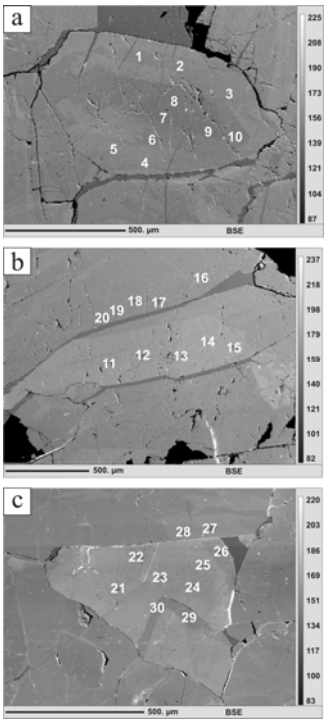

Figure 5. BSE image of three optically zoned hydrothermal tourmalines.

Table 6. Electron microprobe analysis of three zoned tourmaline grains in Figure 5

	Oxide / Point	F	Na_2O	MgO	Al_2O_3	SiO_2	CaO	TiO_2	FeO	Cr_2O_3	MnO	Total	FeO/FeO+MgO	Zone
Grain 1	1	bdl	1.63	7.73	32.45	36.10	1.85	0.65	7.13	0.01	0.06	87.61	0.48	Dark
	2	bdl	1.65	7.88	32.35	35.95	1.91	0.63	7.53	0.01	0.05	87.97	0.49	Dark
	3	bdl	1.67	7.69	32.72	35.93	1.79	0.60	7.34	0.02	0.04	87.89	0.49	Bright
	4	bdl	1.54	7.74	31.58	36.24	2.14	1.01	7.89	0.02	0.06	88.33	0.50	Bright
	5	bdl	1.56	7.63	31.60	35.99	2.13	1.06	8.16	0.02	0.04	88.23	0.52	Bright
	6	bdl	1.75	7.42	33.60	36.66	1.54	0.29	7.04	0.01	0.05	88.41	0.49	Dark
	7	bdl	1.68	7.11	34.28	36.93	1.05	0.04	6.50	0.01	0.04	87.69	0.48	Dark
	8	bdl	1.69	7.19	34.20	37.05	1.06	0.11	6.54	0.01	0.04	87.91	0.48	Dark
	9	bdl	1.61	6.97	34.24	36.87	1.05	0.11	6.64	0.03	0.04	87.62	0.49	Dark
	10	bdl	1.74	6.95	34.18	36.69	1.08	0.13	7.04	0.03	0.04	87.88	0.50	Dark
Grain 2	11	bdl	1.16	7.73	31.15	35.96	2.92	0.78	7.99	0.02	0.05	87.76	0.51	Dark
	12	bdl	1.14	8.05	30.55	36.20	3.14	0.86	8.04	0.04	0.05	88.20	0.50	Bright
	13	bdl	1.10	7.82	30.10	36.07	3.06	1.34	8.67	0.03	0.04	88.25	0.53	Bright
	14	bdl	1.15	7.85	30.35	35.68	2.89	1.52	8.68	0.03	0.06	88.24	0.52	Bright
	15	bdl	1.42	7.69	30.72	35.81	2.40	1.59	8.31	0.02	0.05	88.13	0.52	Bright
	19	bdl	1.59	7.42	32.76	36.42	1.87	0.37	7.67	0.01	0.04	88.23	0.51	Dark
	20	bdl	1.69	7.66	32.62	36.71	1.86	0.48	7.57	0.01	0.05	88.68	0.50	Dark
Grain 3	21	bdl	1.16	8.15	30.64	36.22	3.03	0.90	8.09	0.05	0.04	88.42	0.50	Bright
	22	bdl	1.15	8.19	31.21	36.59	3.06	0.81	7.62	0.04	0.05	88.81	0.48	Bright
	23	bdl	1.26	7.76	30.99	35.98	2.74	0.75	8.24	0.03	0.05	87.85	0.52	Bright
	24	bdl	1.16	8.08	31.33	36.43	2.95	0.81	7.85	0.04	0.05	88.82	0.49	Bright
	25	bdl	1.18	8.09	31.02	36.36	3.01	0.78	8.05	0.03	0.04	88.68	0.50	Bright
	26	bdl	1.67	7.84	32.50	36.72	1.85	0.42	7.43	0.01	0.05	88.52	0.49	Dark
	27	bdl	1.48	7.71	31.75	36.19	2.20	0.88	7.73	0.03	0.05	88.10	0.50	Bright
	28	bdl	1.48	7.86	31.92	36.26	2.27	0.89	7.79	0.03	0.05	88.66	0.50	Bright
	29	bdl	1.62	8.04	31.93	36.13	2.01	0.48	7.26	0.03	0.04	87.53	0.47	Dark
	30	bdl	1.65	7.97	32.14	36.29	2.11	0.46	7.24	0.03	0.05	88.03	0.48	Dark

bdl: Below detection limit which is for F < 1000 ppm.

tourmalines of hydrothermal veins are more dravitic, representing fine-scale chemical and optical zonation. It seems that quartzdioritic rocks of the Boroujerd complex were poor in B, in addition to very low level amounts of P and F. The later is documented by the absence of minerals such as topaz, fluorite and apatite (except invisible small inclusions in tourmaline). These minerals are mostly common in world-known greisen and intrusion-related hydrothermal W-Sn vein systems.

The metaluminous nature of the parent magma and lower activity of Al is believed to have prevented enrichment of melt with respect to B, leading to destablizing and very low amount of tourmaline in the igneous host. Additionally, low level amount of litophile metals (e.g. of the Li-Cs-Ta family) indicates weak to moderate degree of differentiation. The Sm-Nd isotope data reveal a source with a lower Sm/Nd than Chondritic Uniform Reservoir (CHUR) for quartz-dioritic and hydrothermal tourmalines. Based on O isotope data on quartz of hydrothermal quartz-tourmaline veins, magmatic mineralizing fluids with

Table 7. $\delta^{18}O$ values of quartz samples

Sample	$\delta^{18}O$ (‰)	Remark
NZ-12	13.6	Mineralized quartz-tourmaline vein, Hassan Abad tunnel
NZ-13	13.3	Mineralized quartz-tourmaline vein, Jafar Abad tunnel
NZ-35	13.1	Barren quartz-tourmaline vein, Abandoned ore dressing plant
NZ-36	13.8	Mineralized quartz-tourmaline vein, Main tunnel
RV-6	11.9	Barren quartz-tourmaline vein, Revesht tunnel

Table 8. Isotope analyses results of the quartzdioritic rocks and hydrothermal tourmaline

Sample	Sm	Nd	$^{147}Sm/^{144}Nd$	$^{143}Nd/^{144}Nd$	2σ	Age (Ma)	σNd	Rb	Sr	$^{87}Rb/^{86}Sr$	2σ	$^{87}Sr/^{86}Sr$	2σ	Initial $^{87}Sr/^{86}Sr$	$T_{DM\ (Ga)}$
Main phase															
NZ-22	3.617	18.430	0.11864	0.512364	4	51.75	-4.83	140.50	263.30	1.54535	0.839	0.712902	0.000009	0.711766	1.259
NZ-26	3.554	17.020	0.12618	0.512448	6	51.75	-3.24	73.60	315.20	0.67555	0.575	0.707583	0.000004	0.707086	1.221
NZ-27	4.674	23.120	0.12217	0.512283	3	51.75	-6.43	135.60	162.00	2.42305	0.717	0.713837	0.000005	0.712056	1.441
NZ-32	4.410	21.360	0.12482	0.512423	4	51.75	-3.72	82.24	386.70	0.61534	0.723	0.707788	0.000007	0.707336	1.245
Aplite															
NZ-41	1.410	5.910	0.14427	0.512395	3	30.00	-4.54	212.90	113.00	5.45719	0.723	0.721074	0.000007	0.718749	1.653
NZ-43	3.759	17.770	0.12782	0.512347	4	30.00	-5.41	23.27	135.20	0.49809	0.473	0.710374	0.000032	0.710162	1.423
Tourmaline															
NZ-36	3.273	13.270	0.14907	0.512432	2	30.00	-3.84	13.64	191.10	0.20646	0.410	0.707245	0.000005	0.707157	1.689
NZ-13	3.256	12.985	0.14856	0.511635	2	30.00	-3.46	12.88	189.11	0.205666	0.389	0.707123	0.000004	0.707136	1.685

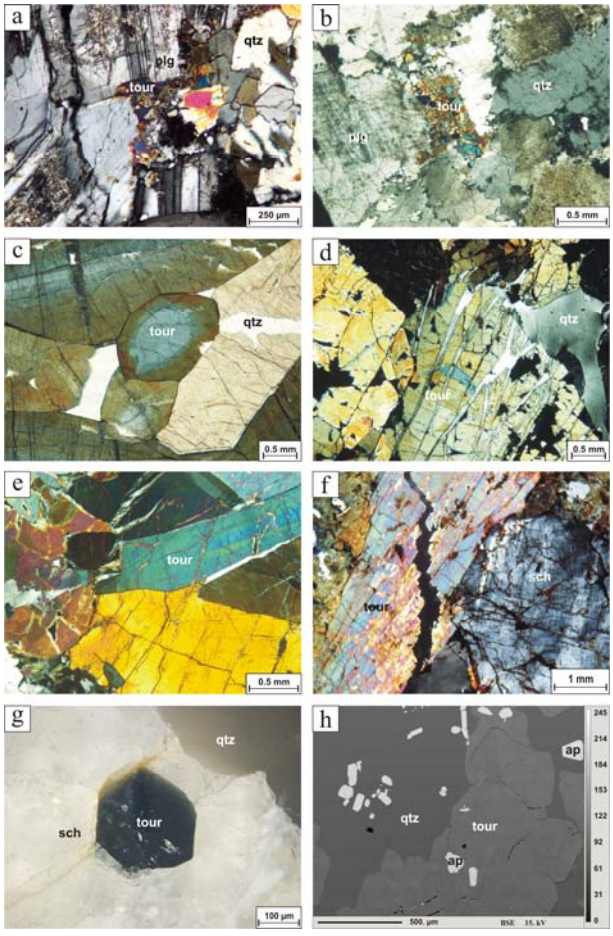

Figure 6. (a & b) Tourmaline in quartrzdiorite, XPL. (c) Zoned tourmaline in hydrothermal quartz vein, XPL. (d) Brecciated tourmaline in hydrothermal quartz vein, XPL. (e) Prismatic zoned tourmaline in hydrothermal quartz vein, XPL. (f) Association of scheelite and zoned brecciated tourmaline in hydrothermal quartz vein, XPL. (g) Euhedral tourmaline in scheelite, PPL, Oil immersion. (h) Apatite inclusion in tourmaline, BSE image.

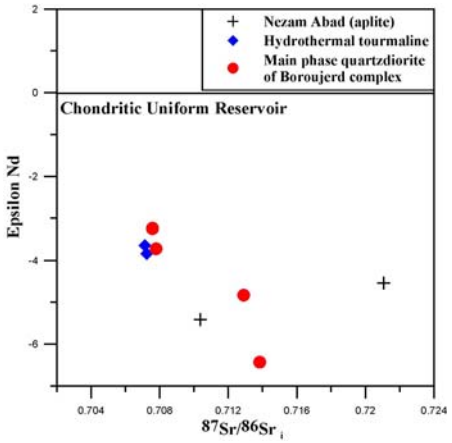

Figure 7. Initial Sr and Nd isotope data for quartzdiorite and tourmaline.

subsequent isotopic exchange with metamorphic country rocks can be inferred. The mentioned veins are related to late-magmatic processes involving the spatially associated quartzdiorite, in which magmatically-derived hydrothermal fluids emanating from the cooling pluton filled dilational fractures and joints created during their emplacement. The current research aimed at study of tourmaline chemistry coupled with former B isotope, petrological and mineralogical data to investigate the evolution of the hydrothermal systems and to constrain its fluids sources. Similar and complementary methods can be used for other B-bearing hydrothermal systems in the country which are associated with different mineralization, particularly W-Sn-(Au) ore deposits.

Acknowledgements

Prof. Andreas Pack is deeply acknowledged for cooperation with O isotope analysis at Goettingen

University, Germany. Klaus Herrmann is highly appreciated for his help with electron microprobe analysis at Technical University of Clausthal, Germany. The authors express their gratitude to Mosab Bazargani for excellent computer assistance. The authors would like to thank two anonymous referees for their helpful comments on the manuscript.

References

1. Agard P., Omrani J., Jolivet L., Mouthereau. Convergence history across Zagros (Iran): Constrains from collisional and earlier deformation. *International Journal of Earth Sciences*, **94**: 401-419 (2005).
2. Ahmad Khalaji A. Peterology of the Granitoid Complex of Boroujerd, PhD *Thesis* (in Persian), University of Tehran, 190 p. (2006).
3. Ahmad Khalaji A., Esmaeily D., Valizadeh M.V., and Rahimpour-Bonab H. Petrology and Geochemistry of the Granitoid Complex of Borougerd, Sanandaj-Sirjan Zone, West Iran. *Journal of Asian Earth Sciences*, **29**: 857-877 (2007).
4. Alavi M. Tectonics of the Zagros orogenic belt of Iran: new data and interpretations. *Tectonophysics*, **229**: 211-238 (1994).
5. Benard F., Moutou P., and Pichavant M. Phase relations of tourmaline lecougranites and the significance of tourmaline in silisic magmas. *Journal of Geology,* **93**: 271-291 (1985).
6. Berberian M. and King G.C.P. Towards a paleogeography and tectonic evolution of Iran. *Canadian Journal of Earth Sciences,* **18**: 210-265 (1981).
7. Deer W.D., Howie R.A., and Zussman J. *An introduction to the rock forming minerals*. 2nd edition. Pearson Education Limited, 150 p (1992).
8. Dingwell D.B., Knocke R., Webb S.L., and Pichavant M. The effect of B_2O_3 on the viscosity of halogranitic liquidus. *American Mineralogist,* **77**: 457-461 (1992).
9. Farhadian M.B. Geochemical and mineralogical investigation on Nezam Abad tungsten deposit, Arak, Iran, M.Sc *Thesis* (in Persian), University of Tehran, 170 p (2003).
10. Faure G. *Principles of Isotope Geology*. John Willey & Sons, 589 p (1986).
11. Gallager V. Geological and isotope studies of microtonalite-hosted W-Sn mineralization in SE Ireland. *Mineralium Deposita,* **24**: 19-28 (1989).
12. Ghasemi A., Talbot C. J. A new tectonic scenario for the Sanandaj-Sirjan zone (Iran). *Journal of Asian Earth Sciences,* **26**: 683-693 (2006).
13. Haghnazar M. Petrogenesis and Nezam Abad Tungsten Mineralization in the South West of Boroujerd Granitoid Complex (West Iran). MSc *Thesis* (in Persian), University of Tehran, 145 p (2007).
14. Haghnazar M., Esmaeily D., and Valizadeh M.V. Origin of tungsten mineralization in the quartzdiorit unit of the Boroujerd Granitoid Complex (Western Iran) using geochemical evidences. *Proc. 17th Goldschmidt Conference, Colegne, Germany, Aug. 19-24*, 367-368 (2007).
15. Haj Zein Ali M.A. Geology and Exploration at Nezam Abad tungsten deposit. *Geological Survey of Iran, Internal report* (in Persian), 40 p (1992).
16. Hoefs J. *Stable Isotope Geochemistry***.** Springer-Verlag, Berlin, 150 p. (2004).
17. Holtz F., and Johannes W. Effect of tourmaline on melt fraction and composition of first melts in quartzofeldspathic gneiss. *European Journal of Mineralogy*, **3**: 527-536 (1991).
18. Icenhower J.P., and London D. In: London D., and Maninng D.A.C. Chemical variation and significance of tourmaline from Southwest England. *Economic Geology*, **90**: 495-519 (1995).
19. Jackson J., and MacKenzie D. Active tectonics of the Alpine-Himalayan belt between western Turkey and Pakistan. *Geophysical Journal of the Royal Astronomical Society*, **77**: 185-264 (1984).
20. Jahangiri H. Investigation into W-Sn anomalies in the areas of Nezam Abad and Bamsar. *Geological Survey of Iran. Internal report* (in Persian), 143 p (1999).
21. Koval P.K., Zorina L.D., Kitajev N.A., Spiridinov A.M., and Ariunbileg S. The use of tourmaline in geochemical prospecting for gold and copper mineralization. *Journal of geochemical exploration*, **40**: 349-360 (1991).
22. Kowsari S. Detailed geochemical exploration of the Shazand Sheet, Scale 1:5000. *Geological Survey of Iran. Internal report* (in Persian)? 203 p. (2004).
23. London D., and Manning A.C. Chemical variation and significance of tourmaline from Southwest England. *Economic Geology*, **90**: 495-519 (1995).
24. Manning D.A.C. Chemical and morphological variation in tourmalines from the Hub Kapong batholith of peninsular Thailand. *Mineralogical Magazine*, **45**: 139-147 (1982).
25. Masoudi F. Contact metamorphism and pegmatite development in the region SW of Arak, Iran, PhD *Thesis*, University of Leeds, 231 p. (1997).
26. Mohajjel M., Fergusson B.C.L. and Sahandi M.R. Cretaceous-Tertiary convergence and continental collision, Sanandaj-Sirjan Zone, western Iran. *Journal of Asian Earth Sciences*, **21**: 397-412 (2003).
27. Nezafati N. Au-W-Sn-Cu mineralization in the Astaneh-Sarband area, west central Iran, PhD *Thesis*, Tübingen University, 116 p. (2006).
28. Puziewicz J., and Johannes W. Phase equilibria and compositions of Fe-Mg-Al minerals and melts in water-saturated peraluminous granitic systems. *Contributions to Mineralogy and Petrology*, **100**: 300-324 (1990).
29. Radfar J. Petrology of granitic rocks from Astaneh area, Iran, MSc *Thesis* (in Persian), University of Tehran, 111 p. (1987).
30. Rollinson H. Using geochemical data: evaluation, presentation, interpretation. Langman Group UK Limited, 352 p. (1993).
31. Shamanian Esfahani G. Geochemical, mineralogical and fluid inclusion studies on Nezam Abad tungsten mine, Markazi province, Iran, MSc *Thesis* (in Persian), University of Shiraz, 212 p. (1994).
32. Stöcklin J. Structural history and tectonics of Iran, a review. *American Association of Petroleum Geologists Bulletin*, **52**(7): 1229-1258 (1968).